Hydrogel/Nanofiber Composite Wound Dressing Optimized for Skin Layer Regeneration through the Mechanotransduction-Based Microcellular Environment

Changgi Hong,[#] Haeun Chung,[#] Gyubok Lee, Changheon Kim, Dongwoo Kim, Seung Ja Oh, Sang-Heon Kim,* and Kangwon Lee*

Cite This: https://doi.org/10.1021/acsabm.3c00014

Read Online

ACCESS | Metrics & More | Article Recommendations | Supporting Information

ABSTRACT: Wound dressings have been designed to provide the optimal environment to fibroblasts, keratinocytes, and macrophages to promote wound healing while inhibiting potential microbial infection. Gelatin methacrylate (GelMA) is a photopolymerizable hydrogel with a gelatin backbone that contains natural cell binding motifs such as arginine–glycine–aspartic acid (RGD) and MMP-sensitive degradation sites, making it an ideal material for wound dressing. However, GelMA alone is unable to stably protect the wound and regulate cellular activities due to its weak mechanical properties and nonmicropatterned surface, limiting its application as a wound dressing. Herein, we report the development of a hydrogel–nanofiber composite wound dressing utilizing GelMA and poly(caprolactone) (PCL)/gelatin nanofiber, which can systematically manage the skin regeneration process with an enhanced mechanical property and micropatterned surface. GelMA sandwiched between electrospun aligned and interlaced nanofibers that mimic epidermis and dermis layers, respectively, increased the stiffness of the resulting hydrogel composite with a comparable swelling rate as GelMA. Fabricated hydrogel composite was determined to be biocompatible and nontoxic. In addition to the beneficial effect of GelMA in accelerating wound healing, subsequent histological analysis revealed upregulated re-epithelialization of granulation tissue and deposition of mature collagen. Hydrogel composite interacted with fibroblasts to regulate their morphology, proliferation, and collagen synthesis, as well as the expression of α-SMA, TGF-β, and collagen I and III during the wound healing process both *in vitro* and *in vivo*. Taken together, we propose hydrogel/nanofiber composite as a wound dressing of the next generation that can induce skin tissue layer regeneration beyond the basic wound closure promotion of present dressings.

KEYWORDS: GelMA, gelatin, PCL, wound healing, wound dressing, nanofiber, mechanotransduction
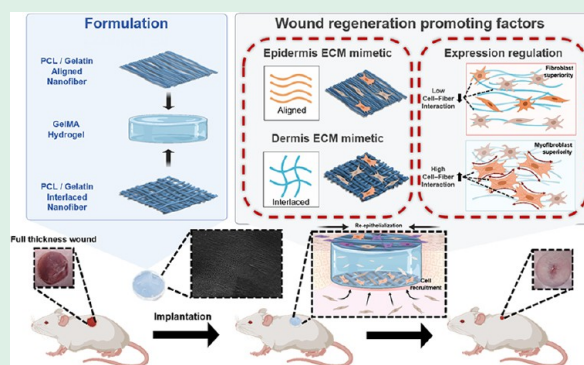
1. INTRODUCTION

The hydrogel wound dressing that provides physicochemical cues essential for tissue homeostasis, morphogenesis, and differentiation with adequate mechanical properties is an ideal candidate for promoting regeneration of the elaborate compositional and architectural characteristics of the native extracellular matrix (ECM).[1,2] Nature-derived hydrogels are extensively used for wound dressing, as their morphological properties and composition can be tuned to mimic the native features of ECM, where appropriate physical and chemical signals can be transmitted to the wound-healing-related cells during the regeneration process.[3−5] However, a fundamental disadvantage of polymers derived from natural sources used in wound dressing applications is their weak mechanical stability, frequently being damaged by friction. In addition, hydrogel derived from nature can only upregulate the cellular activities of protein synthesis that promote wound contraction but cannot effectively manage the matrix remodeling process,

which is the longest step in the wound healing process and is the essential step in restoring its normal function.[6] For these reasons, developing a novel nature-derived hydrogel wound dressing with tunable mechanical modulus and biological-guiding micropatterns is vital for skin tissue engineering applications.

The most promising candidate for the fabrication of wound dressings is gelatin methacrylate (GelMA) hydrogels, which possess the benefits of both natural and synthetic biomaterials. GelMA hydrogels have gelatin as their backbone, which offers them cell-responsive capabilities, such as appropriate cell
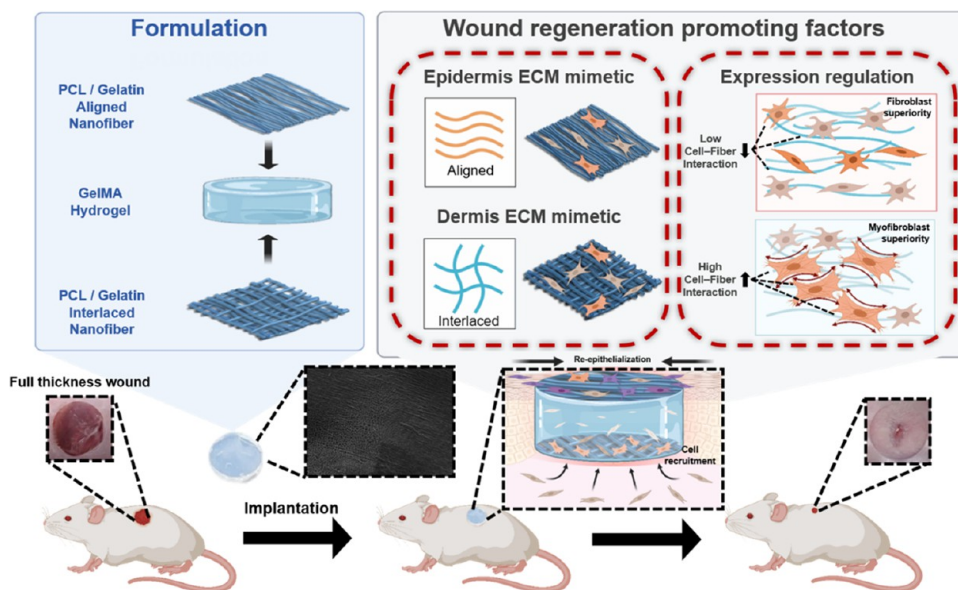
Figure 1. Schematic illustration of skin-mimetic hydrogel composite wound dressing for mechanotransduction-based wound regeneration. Aligned and interlaced nanofibers were coated with GelMA hydrogel, maximizing the wound regeneration efficiency by simultaneously controlling the expression and arrangement of cells. Figures were created with BioRender.com.

adhesion sites and proteolytic degradability, as well as the ability to trigger cell migration and angiogenesis *in vivo.*[7,8] Augustine and co-workers showed that GelMA hydrogel containing cerium oxide nanoparticles promoted the healing of diabetic wounds successfully owing to its adequate fluid capacity, degradability, and antioxidant activity.[9] Despite the outstanding performance of GelMA hydrogel, strong cross-linking of GelMA has downsides such as cytotoxicity, gas exchange limitation, and inability to adequately absorb exudate, limiting its application as wound dressings.[10] Additionally, GelMA hydrogel cannot stimulate cells to reconstruct the skin layer inside the granular tissue during the matrix remodeling process.

Recently, research has been conducted on utilizing mechanotransduction to facilitate the matrix remodeling process from the early wound healing step by controlling the mechanical characteristics such as organization, composition, and porosity of the scaffold where cells interact.[6,11−13] During wound healing, mechanosensitive cells in the skin such as fibroblasts and keratinocytes respond to the external environment by modifying their shape, migrating, proliferating, differentiating, and engaging in other biological actions.[14−17] Since the architectural characteristics of the scaffold have a substantial influence on the matrix remodeling process, skin regeneration can be enhanced by adjusting and giving optimal mechanical conditions to cells for wound healing.

In this paper, a wound dressing composed of poly-(caprolactone) (PCL)/gelatin nanofibers embedded in GelMA hydrogel was developed to mimic the natural skin layer and control cell activation through mechanotransduction (Figure 1). In this hydrogel composite, the composition and orientation of the nanofibers were tuned to designate the cell's activity and morphology. Thus, we hypothesized that incorporating PCL/gelatin nanofiber into GelMA hydrogels would engineer biocompatible scaffolds with improved mechanical strength and intrinsic bioactivity for tissue engineering. We demonstrated that the hydrogel composite displayed excellent mechanical properties *in vitro*, making it

possible to use it extensively as a wound dressing. The therapeutic effect of the hydrogel composite was observed through a full-thickness wound *in vivo* test, and it showed rapid re-epithelialization and collagen maturation as well as a significant acceleration of the ECM remodeling process. Through our findings, it was indicated that the hydrogel/nanofiber composite wound dressing can be utilized to encourage wound regeneration and restore healthy skin.

2. MATERIALS AND METHODS

2.1. Materials. Gelatin (type A, G2500), poly(caprolactone) (PCL, M_n = 80,000), methacrylic anhydride, 2,2,2-trifluoroethanol-(2,2,2-TFE), 2-hydroxy-40-(2-hydroxyethoxy)-2-methylpropiophenone (Irgacure 2959, 98% purity), and 4′,6-diamidino-2-phenylindole were all acquired from Sigma-Aldrich (St Louis, MO). Acetic acid (glacial, 99.5%) was obtained from Samchun Chemical Co., Ltd. (Pyeongtaek, South Korea). LIVE/DEAD was obtained from Thermo Fisher Scientific (Waltham, MA). Alexa Fluor 488 Phalloidin was purchased from Invitrogen (Waltham, MA). Dojindo Laboratories provided the Cell Counting Kit-8 (CCK-8) (Tokyo, Japan). 4% Paraformaldehyde was acquired from Biosesang (Seongnam, South Korea), and phosphate-buffered saline (PBS) and Dulbecco's modified Eagle's medium (DMEM) were supplied by Welgene Inc. (Seoul, South Korea). Fetal bovine serum (FBS) was obtained from CellSera (Rutherford, Australia).

2.2. Synthesis of Gelatin Methacrylate Hydrogel. GelMA was prepared by following previously published methods.[18] After preparing 10% (w/v) gelatin stock solution in PBS, methacrylic anhydride was mixed gently into the gelatin solution at a weight ratio of 1:1.7 (gelatin/methacrylic anhydride) and reacted at 50 °C with steady stirring for 1 h. Next, the solution was dialyzed against deionized water for 3 days to remove the unreacted methacrylic anhydride. The GelMA solution was lyophilized under sterile conditions. To prepare GelMA hydrogel, 10% (w/v) lyophilized GelMA and 0.2% (w/v) irgacure were dissolved in PBS.

2.3. Characterization of Gelatin Methacrylate Hydrogel. To examine the chemical composition of synthesized GelMA, Fourier transform infrared (FTIR) spectra of the dried gelatin and GelMA hydrogel were recorded within a frequency range of 400−4000 cm^{-1} at 25 °C using a Fourier transform infrared (FTIR) spectrometer (ALPHA, Bruker, MA).

The degree of functionalization of synthesized GelMA was calculated according to the previously reported method.[18] Briefly, standards and samples were added to a 96-well plate and mixed with 12 mM ninhydrin: 100% ethanol (1:8 ratio) solution. The plate was incubated at 70 °C for 1 h for color development, and the absorbance was measured at 570 nm using a spectrophotometer (Synergy H1, BioTek Instruments, Winooski, VT). Gelatin hydrogel prepared at concentrations ranging from 0 to 10 mg/mL was used to establish a standard curve. GelMA at a concentration of 10 mg/mL was then used to measure the degree of functionalization.

2.4. Synthesis and Characterization of the Electrospun Nanofibers. Stock solutions of PCL (10%, w/v) and gelatin (10%, w/v) were prepared by dissolving it in 2,2,2-trifluoroethanol: acetic acid (9:1) solution with vigorous stirring at 25 °C overnight. PCL/gelatin solutions were prepared at different ratios (10:0, 8:2, 6:4) and transferred to a syringe for electrospinning (ESR100, NanoNC, Seoul, South Korea). Electrospinning was performed for 2 h at the following parameters: temperature at 37 °C, an applied voltage of 13 kV, constant flow rate at 0.3 mL/h, and a distance of 15 cm between the 25-gauge needle tip and aluminum foil. A cylindrical collector with a diameter of 8 cm and a rotating speed of 3000 rpm was used to collect the electrospun fibers. To collect aligned nanofiber, a cylindrical collector was left undisturbed, and to collect interlaced nanofiber, the aluminum foil was rotated 90° every 30 min.

The uniformity of orientation of the collected nanofibers was examined using scanning electron microscopy (SEM, SNE-4500M, NanoImages, LLC, Pleasanton, CA). To prepare samples for SEM, collected electrospun aligned and interlaced PCL/gelatin nanofibers were dried at 37 °C on a clean aluminum foil and coated with platinum using an ion sputter coater (MCM-100, SEC Co. Ltd, Suwon, South Korea). The orientation coherency and diameter of nanofibers were analyzed using ImageJ software (ImageJ, Bethesda, MD) with OrientationJ plugin.

2.5. Synthesis and Characterization of the Hydrogel Composite. Nanofibers produced by the method as described above were washed with 70% (w/v) ethanol and dried under an ultraviolet (UV) lamp for 1 h for sterilization. After sterilization, the nanofibers were immersed in DMEM media overnight to increase the hydrophilicity of nanofibers. After the flattening of the interlaced nanofiber layer, 1 mL of a preheated GelMA solution was injected into the mold. The aligned nanofiber layer was then delicately placed over the GelMA solution, stamped horizontally using a stamper to synthesize a 1mm thick hydrogel composite, and UV-crosslinked for 5 min at 365 nm using a UVP crosslinker (CL-1000, Analytik Jena AG, Jena, Germany) (Figure S1a). To determine the thickness of nanofibers, fibroblasts were cultivated for 24 h on aligned and interlaced nanofibers, and the height difference at which the cells were dispersed was used to measure nanofiber thickness.

The cell nuclei were stained with DAPI, and confocal laser spectroscopy was used to analyze Z-stack pictures of fibroblasts. The thickness of each nanofiber was estimated to be around 100 μm under both arrangements, with the interlaced layer showing a slightly thicker aspect than the aligned layer due to greater fiber stacking (Figure S1b).

GelMA weighed 0.052 g, and nanofiber weighed 0.0012 g, yielding a weight ratio of 43:1 for the hydrogel wound composite.

The viscoelastic characteristics of the scaffolds were determined using dynamic shear modulus deformation analysis. Samples were placed between a 2 cm metal plate with a 1 cm gap, and their vibration-shear deformation was evaluated using a rheometer (MCR 102, Anton Paar, Graz, Australia). The storage modulus was determined under continuous deformation mode with 10% constant strain maintained across a frequency range of 0.1−300 Hz (rad/s) at 25 °C.

The swelling capacity of the hydrogels was determined by measuring the weight change at various time points at 37 °C. Hydrogel samples were freeze-dried prior to the swelling test and swollen in PBS buffer. Before measuring weight, the excess PBS on the surface of the hydrogel was absorbed with filter paper and accurately weighed in triplicate. The swelling ratio (SR) was calculated according to the formula $(W_t - W_0)/W_0 \times 100$.[19]

2.6. Cell Culture. The experiment was performed using human fibroblasts (CCD-986sk cell line, Korean Cell Line Bank, Seoul, South Korea). Fibroblasts were cultured in high-glucose DMEM supplemented with 10% (v/v) FBS and 1% (v/v) penicillin−streptomycin in an incubator set to 37 °C and 5% CO_2. Media was changed every 2 or 3 days. Experiments were performed at passage 4.

Human monocytic cell lines THP-1 (TIB-202, American Type Culture Collection, Rockville, MD) were cultured in Roswell Park Memorial Institute (RPMI) medium supplemented with 10% FBS and 1% (v/v) penicillin−streptomycin. Macrophage M0 was polarized from THP-1 treated PMA (50 μg/mL) for 48 h.

Human Epidermal keratinocyte cells (CB-HK-001, Cefobio, Gyeonggi-do, Korea) were cultured in Keratinocyte Growth Medium 2 kit (PromoCell, Germany). Experiments were performed at passage 4.

2.7. Cytotoxicity Assay. The cytotoxicity of hydrogel composite on fibroblasts was measured indirectly using hydrogel extracts, following ISO 10993-12 method.[20] Briefly, hydrogel extracts were prepared by swelling the hydrogel composite in DMEM at a concentration of 0.2 g/mL in an incubator for 24 h at 37 °C. The extracted solution was diluted with free DMEM from 100 to 12.5% every twofold. Free DMEM was included as a negative control.

For the CCK-8 assay, human fibroblasts were seeded at a density of 5×10^4 cells per well in 96-well plates and incubated for 24 h. After removing the media, fibroblasts were treated with diluted hydrogel extracts for 1 or 4 days in a 37 °C incubator with 5% CO_2. The viability of the cells was determined on days 1 and 4 using the Cell Counting Kit-8 (CCK-8). Briefly, CCK-8 solution was added to each well and incubated for 2 h, and the absorbance was measured at 450 nm using a microplate reader (Synergy H1, BioTek, VT).

For LIVE/DEAD assay, human fibroblasts were seeded at a density of 3×10^4 cells per well on 24-well plates for 24 h. After treating the cells with hydrogel extract solution in the same manner as described above, the cell viability at day 1 and 4 were observed by adding live and dead reagents for 45 min in the dark at 25 °C. Images of fibroblasts were taken using a fluorescent microscope (Axio Observer Z1, Carl Zeiss, Oberkochen, Germany).

2.8. Quantitative Real-Time Polymerase Chain Reaction (qRT-PCR). Fibroblasts were cultured on different arrangements (aligned, interlaced), and compositions of nanofibers (10:0, 8:2, 6:4; PCL/gelatin ratio) were cultured for 1 or 4 days, and their total RNA was extracted using the TRIzol method. Total RNA was reverse-transcribed to cDNA, and qRT-PCR was performed using the SYBR Green system (Thermo Fisher, Waltham, MA) and QuantStudio 5 system (Applied Biosystems, Waltham, MA) as per the manufacturer's protocol. The expressions of type I collagen, type III collagen, and α-SMA were normalized against the housekeeping gene, glyceraldehyde-3-phosphate dehydrogenase (GAPDH). Sequences of the primers for the various genes are listed in Figure S2.

2.9. Animal Care. Seven-week-old male BALB/c mice were supplied by Orient Bio Inc. (Seongnam, South Korea) and were allowed to acclimate for at least 1 week prior to surgery. Mice were housed in a room maintained at a temperature of 25 °C with a 12 h light/dark cycle and were given free access to food and water. All procedures involving animals were approved and in compliance with the ethical regulations set out by the Korea Institute of Science and Technology's International Animal Care and Use Committee [KIST-2021-021].

2.10. Surgical Procedures and Implantation of the Scaffold. Before surgery, mice were put under anesthesia by isoflurane inhalation, and their hair was removed. Two full-thickness excisional skin wounds were created on each side along the midline of the dorsal region of each mouse using an 8 mm biopsy punch. To prevent wounds from contracting, silicon ring splints were glued onto the edges of the wound using Krazy glue. Mice were randomly divided into 3 groups (n = 9/group) and received no treatment (control group), GelMA, or hydrogel composite that were pre-cut into circular patches 10 mm in diameter. After placing wound dressing over the
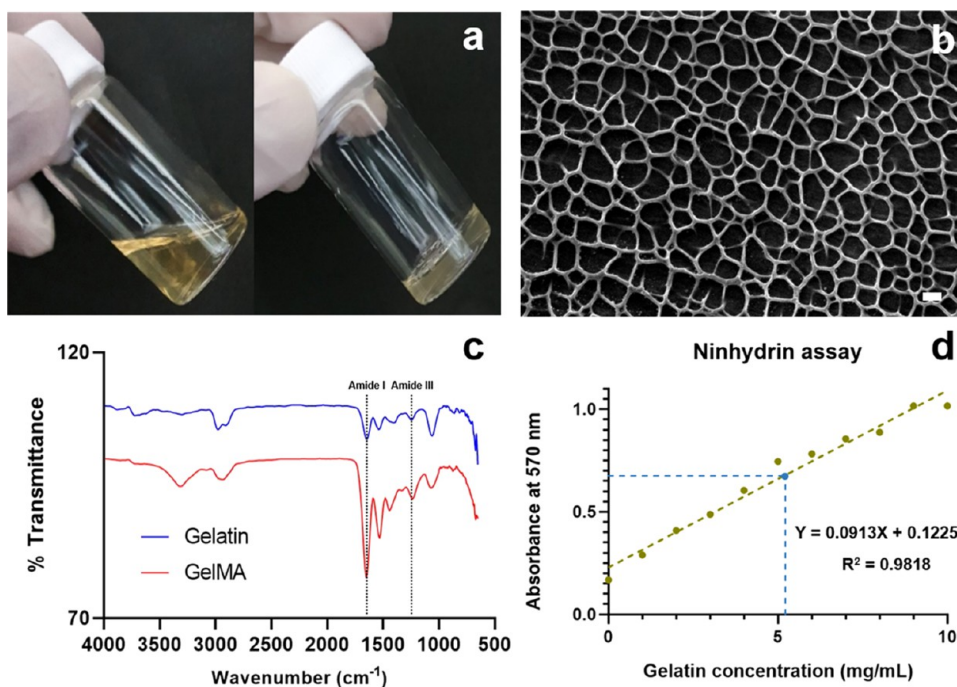
Figure 2. Digital photographs of before and after UV crosslinking of the GelMA hydrogel solution (a); representative SEM image of lyophilized GelMA (b). Scale bar: 10 μm; FTIR spectra of the gelatin and GelMA scaffolds (c); determination of degree of functionalization of synthesized GelMA by ninhydrin assay (d).

wounds, all wounds were covered with Tegaderm (3M Healthcare) and then strapped with a band-aid. Mice from each group (n = 3) were sacrificed 3, 7, and 14 days after the surgery, and skin tissues were collected for immunofluorescence and histological analysis.

Digital images of the wound regions on days 0, 3, 7, and 14 were used to determine the wound healing state of each group. The area of the wounds was analyzed using ImageJ software (ImageJ, Bethesda, MD). The wound healing rate was determined using the following formula: $(A_0 - A_t)/A_0 \times 100\%$, where A_0 is the initial wound area and A_t is the wound area at time t.

2.11. Histological Evaluation. After euthanasia, skin tissue was harvested on day 14 for histological evaluation. Samples were fixed in 10% (w/v) neutral buffered formalin, dehydrated, and prepared into paraffin blocks. 10 μm thick paraffin sections were made, deparaffinized, and rehydrated. Prepared slides were then stained with hematoxylin−eosin, Masson's trichrome, and Herovici stain solution for histological analysis. An Axio Vert1 A1 phase contrast microscope was used to capture images of the tissue slices (Zeiss, Oberkochen, Germany).

2.12. Immunofluorescence. For Immunofluorescent staining, samples were fixed with 4% paraformaldehyde, blocked in blocking solution (1% bovine serum albumin + 0.1% Titon X-100 in PBS) for 1 h at 25 °C, and incubated with primary antibodies diluted in blocking solution for overnight at 4 °C. After washing, samples were incubated with secondary antibodies diluted in blocking solution for 2 h at 25 °C and mounted with Vectashield mounting medium containing DAPI (Vector Laboratories, Inc., Newark, CA). To investigate F-actin and morphological changes of cells on nanofibers, each nanofiber was first affixed to a Petri dish for cell culture, and then an equal number of fibroblasts, macrophages, and keratinocytes were implanted and cultured for 24 h. Images were taken using a fluorescence spectroscope (Axio Observer, Carl Zeiss, Oberkochen, Germany). Antibodies and dilutions used for the experiment are listed in Figure S3.

2.13. Statistical Analysis. All data were reported as the mean ± standard deviation. Data were analyzed using GraphPad Prism 8 software (GraphPad, San Diego, CA). Comparison between groups was performed using one-way ANOVA, followed by multiple comparison tests at a confidence level of 95%. *P*-values less than 0.05 were indicated as statistically significant.

3. RESULTS AND DISCUSSION

3.1. Fabrication and Characterization of the GelMA Hydrogel. GelMA is a biocompatible and biodegradable substance synthesized from gelatin, which is a hydrolyzed form of collagen, a major component of skin, and a very suitable material for the activation of fibroblasts, keratinocytes, and macrophages.[7,8] In addition, GelMA may also be liquified in mild conditions and can be processed into desired shapes when exposed to UV light, making it suitable for its use as a scaffold (Figure 2a). Furthermore, the pore size of the lyophilized GelMA was 87 ± 8 μm, which is adequate for cell proliferation and migration (Figure 2b).[21,22]

The FTIR spectra of pure gelatin and synthesized GelMA were analyzed to check that the methacrylate group was sequentially bound to the gelatin (Figure 2c). First, there was a reduction in the peak near 3300 cm^{-1} owing to UV crosslinking of GelMA, which decreased the overall amount of −OH groups in the structure.[23] The characteristic amide l and II bands at 1640 and 1540 cm^{-1} (owing to C=O stretching and N−H bending, respectively) are present in all of the materials, although their intensities are greater in GelMA due to its crosslinked structure.[24] In addition, GelMA displays a sharper intensity peak in the Amide III (1250−1350 cm^{-1}) peak region, which corresponds to the in-plane bending of the −CH$_2$ in the protein backbone.[25] The increased intensity of this peak in GelMA is due to the crosslinking of the protein backbone by methacrylate groups, which creates a more rigid material structure.

The density of the amine groups in the GelMA solution was quantified utilizing a colorimetric ninhydrin test to determine the degree of functionalization (Figure 2d). The results revealed that the degree of functionalization was 47% when
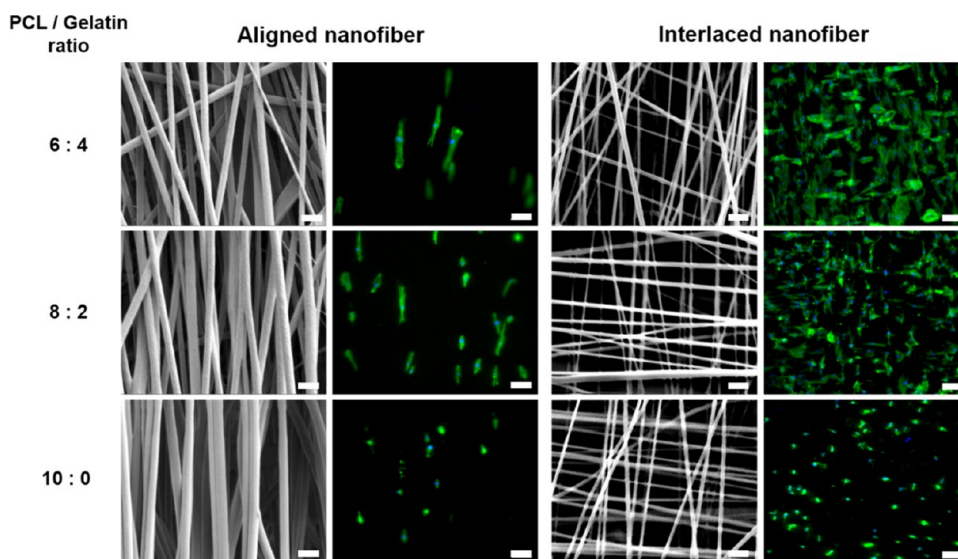
Figure 3. SEM images of electrospun nanofibers prepared at 6:4, 8:2, and 10:0 ratios (PCL/gelatin). Scale bar: 1 and 2 μm for aligned and interlaced, respectively; fluorescent images showing the morphology of fibroblasts cultured on the nanofiber scaffolds for 24 h. F-actin (green), nuclei (blue). Scale bar: 100 μm.

the GelMA value is substituted into the standard curve, which is a value sufficient to form a scaffold through photocrosslinking.[26]

3.2. Fabrication and Characterization of the Electrospun Nanofibers. PCL is a synthetic polymer that is linear and hydrophobic and has a high mechanical strength. While PCL nanofibers may structurally resemble the ECM as in biological tissues, their low hydrophilicity impairs their capacity to promote cell adhesion, migration, proliferation, and differentiation. Gelatin, by contrast, retains the arginine-glycine–aspartic acid (RGD) sequence, which helps cells to adhere, differentiate, and proliferate. Taken together, gelatin and PCL can be combined to create a nanofiber that is biocompatible and mechanically stable.[27] We hypothesized that mechanotransduction-based interactions between the nanofibers and fibroblasts may restore the intricate organization of the skin layer by stimulating cell growth along the structure of the arrayed nanofibers. Especially in hypertrophic scars, the matrix remodeling process does not progress properly, resulting in a haphazard arrangement of collagen that leads to scar development and inferior strength. Accordingly, if a scaffold can replicate the structure of normal collagen organization to induce cell arrangement from the early stage of the repairing process, the duration of ECM remodeling phase can be reduced, and the scar formation can be inhibited.

Because the density, composition, and orientation of the nanofibers can significantly influence the degree of interaction between the cells and nanofibers, nanofibers with various PCL/gelatin ratios (10:0, 8:2, and 6:4) and configurations (aligned or interlaced) were electrospun, and their effect on fibroblasts were examined. It was determined that when the gelatin content surpassed 6:4, the electrospinning solution's low viscosity during the electrospinning process rendered it difficult to produce nanofibers with a consistent diameter and alignment. In previous publications, it has been proven that nanofibers of irregular diameter are generated when the ratio of PCL to gelatin surpasses 6:4.[28,29] To study the interaction with cells based on the composition and arrangement of nanofibers under more consistent settings, the condition with the

maximum interaction with cells was set to 6:4, the group with the lowest contact with cells was set to 10:0, and the medium value was set to 8:2.

The surface of the nanofibers prepared with each composition was observed through SEM images (Figure 3). Nanofibers were produced uniformly and smoothly without beading or branching, which hinders the interaction between the cells and the nanofibers. The nanofiber diameter was reduced when the gelatin content in the solution was increased due to the decreasing viscosity. Still, the nanofibers provided enough area for fibroblasts to adhere and proliferate under all conditions (Figure S4).[27]

Nanofibrous scaffolds with interlaced spatial configurations were produced by altering the orientation of the aluminum foil on the drum collector. The SEM image shows that most of the nanofibers collected on the drum collector are oriented in a uniaxial distribution. The diameter of the interlaced nanofibers prepared at 10:0, 8:2, and 6:4 ratios (PCL/gelatin) were 413 ± 58, 332 ± 53, and 283 ± 60 nm, respectively. In contrast, there was no significant difference in the diameter of the electrospun nanofibers, regardless of the arrangement tested. Moreover, the fiber orientation analysis confirmed that more than 90% of the nanofibers were arranged as intended (Figure S5).

3.3. Optimal PCL/Gelatin Composition According to the Nanofiber Arrangement. The skin is classified into three layers, dermis, epidermis, and subcutaneous tissue, based on functional and anatomical differences.[30] The dermis and epidermis are the two primary layers of the skin, with keratinocytes and fibroblasts mainly determining the protein composition, orientation, and structure of each layer. Collagen fibrils are the primary ECM components of the epidermis and dermis, and they are specifically arranged (aligned and interlaced, respectively) to improve their physical functions (load-bearing, friction reduction, osmotic power, stiffness, and cell proliferation).[31] To avoid a poor prognosis or the formation of scars, ideal wound healing seeks to restore the intricate structure of the skin while managing cellular repair processes.
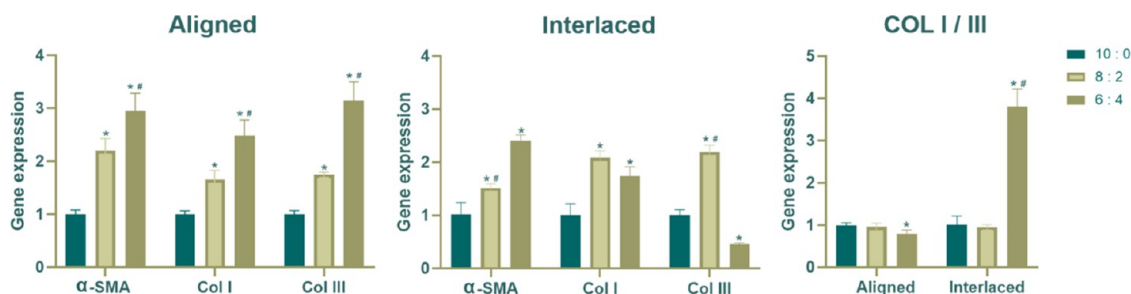
Figure 4. Gene expression of fibroblasts cultured on nanofibers. Fibroblasts were cultured on an aligned and interlaced nanofibrous scaffold with varying PCL: gelatin ratios for 4 days and its gene expression were analyzed by qRT-PCR. All values were normalized to GAPDH. Data are mean ± SD. *$p < 0.05$ against 10:0 group; #$p < 0.05$ against 8:2 group in Aligned and 6:4 in Interlaced.

In vivo, cells perceive the physical constraints of their surroundings through the integrin-cytoskeleton-nuclei membrane linkage and convey the signal *via* the Hippo and Wnt signal pathways, which control cell migration, growth, and expression during wound healing.[32] Furthermore, the arrangement of ECM-related proteins produced by cells according to the cell arrangement also acts as a feedback loop that affects cell activity. The mechanical strength and the osmotic and nutritional gradients of the surrounding ECM are determined by the protein arrangement, resulting in a difference in expression depending on the location of cells in the tissue, which becomes a trigger to produce a specific tissue.

When a wound occurs, migration of the cells begins in the skin tissue around the wound and through the circulatory system.[18,33−35] Cell migration proceeds with stretching along with the ECM to which cells are attached, and the cell morphology changed by the stretching is accompanied by cytoskeletal adaptation. The nuclear pore size is increased by tension in the cytoskeleton-nucleus membrane connection, and the expression of TGF-β1 signaling molecules is accelerated, increasing the differentiation of fibroblasts into myofibroblasts, which act as mediators in wound contraction, collagen manufacture, and keratinocyte activation.

Aberrant expression of myofibroblast is a direct factor in chronic wound and scar formation, demonstrating its importance in the wound healing process. Therefore, fluorescence staining and qPCR analysis were performed to determine the optimal PCL/gelatin composition for each arrangement that mimics the epidermis and dermis.

3.3.1. Immunofluorescent Staining of the Cell Morphology. An aim of this paper was to induce proper regeneration of skin tissue at the wound site by controlling the proliferation and migration of fibroblasts through the hydrogel composite wound dressing. The morphology of the fibroblasts grown on the nanofibers was analyzed by immunostaining to demonstrate that cell development growth and differentiation can be regulated by the interaction with the nanofibers. In Figure 3, we observed how the growth of fibroblasts was induced on the nanofiber scaffolds made of different proportions of gelatin. In contrast to PCL, gelatin is a naturally derived material, and it contains the Arg−Gly−Asp (RGD) sequence, enabling fibroblasts to attach to and grow along the nanofibers. When the PCL/gelatin ratio was changed from 10:0 to 6:4, the anchorage points of the fibroblasts on the nanofiber scaffold increased. Consequently, the fluorescence images of the fibroblasts grown for 24 h at each composition showed that elongation and migration of the fibroblasts were promoted as the gelatin content in the nanofibers was increased both in the aligned and interlaced forms. Interestingly, on nanofibers comprised entirely of PCL, the fibroblasts could not grow by attaching to the surface; thus, they had a round shape as in the initial state of the cell seeding process. Additionally, it was revealed that the morphology of the cells can be controlled according to the composition of the mixed synthetic PCL and natural gelatin and that it can induce cell behavior during wound healing through mechanotransduction. Furthermore, the gelatin-containing nanofibers were also able to induce cell migration and elongation by following their arrangement, thereby mimicking the intrinsic arrangement of the ECM within the skin layer.[30,36]

In addition to fibroblasts which were the focus of this study, keratinocytes and macrophages also play a significant role in wound healing. Macrophages and keratinocytes were cultivated on aligned and interlaced nanofibers to determine whether cell morphology differs based on nanofiber composition (Figure S6). According to the fluorescent images, the morphology of macrophages and keratinocytes altered based on the composition and arrangement of nanofibers. Similar to fibroblasts, the interaction level with cells can be regulated by increasing or lowering the anchoring site on the nanofiber, and cell growth and expression could be promoted by the transmission of mechanotransduction signals.[17,37]

3.3.2. PCR Analysis. Differences in fibroblast gene expression were examined using PCR analysis in relation to the composition and arrangement of the nanofibers (Figure 4). The PCR results determined the most suitable PCL/gelatin ratio in an aligned and interlaced nanofiber that mimics the epidermis and dermis layers, respectively.[6,13] Fibroblasts were cultured on nanofiber meshes for 1 or 4 days, and gene expression levels of fibroblasts related to wound healing markers were examined. GAPDH was used as a housekeeping gene, while marker genes (α-SMA, Col I, and Col III) were used to standardize the degree of fibroblast differentiation into myofibroblasts. In both the aligned and interlaced nanofibers, there was no significant difference in gene expression according to the composition after 24 h (Figure S7). Cells require time to become firmly attached to the nanofibers, and then, they begin to express elongation, proliferation, migration, and differentiation factors in different manners depending on the chemical properties of the surface. Surprisingly, the composition and arrangement of the nanofibers had a great effect on cell activation, changing the degree of myofibroblast differentiation and the production and ratio of collagen I and III after 4 days.

During wound healing, myofibroblasts are cells that promote wound contraction and collagen synthesis, and the expression of collagen I and III increased in proportion to changes in α-SMA expression. To successively promote wound healing by
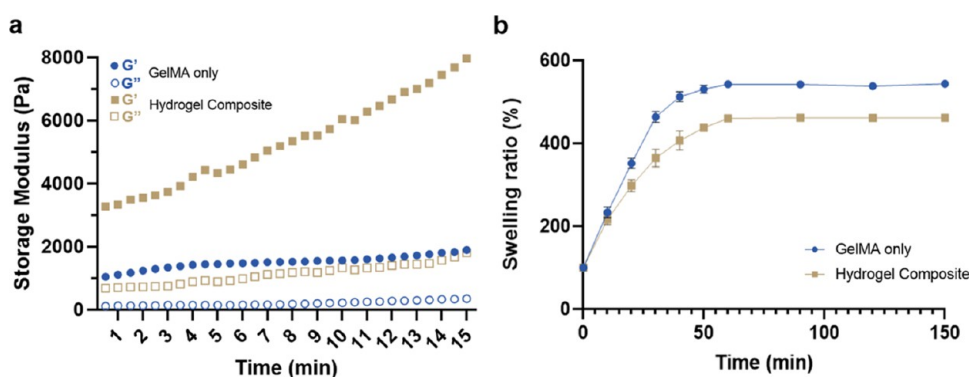
Figure 5. Dynamic mechanical properties of the GelMA and hydrogel composites (a); swelling ratio of the hydrogels at different swelling intervals (b).
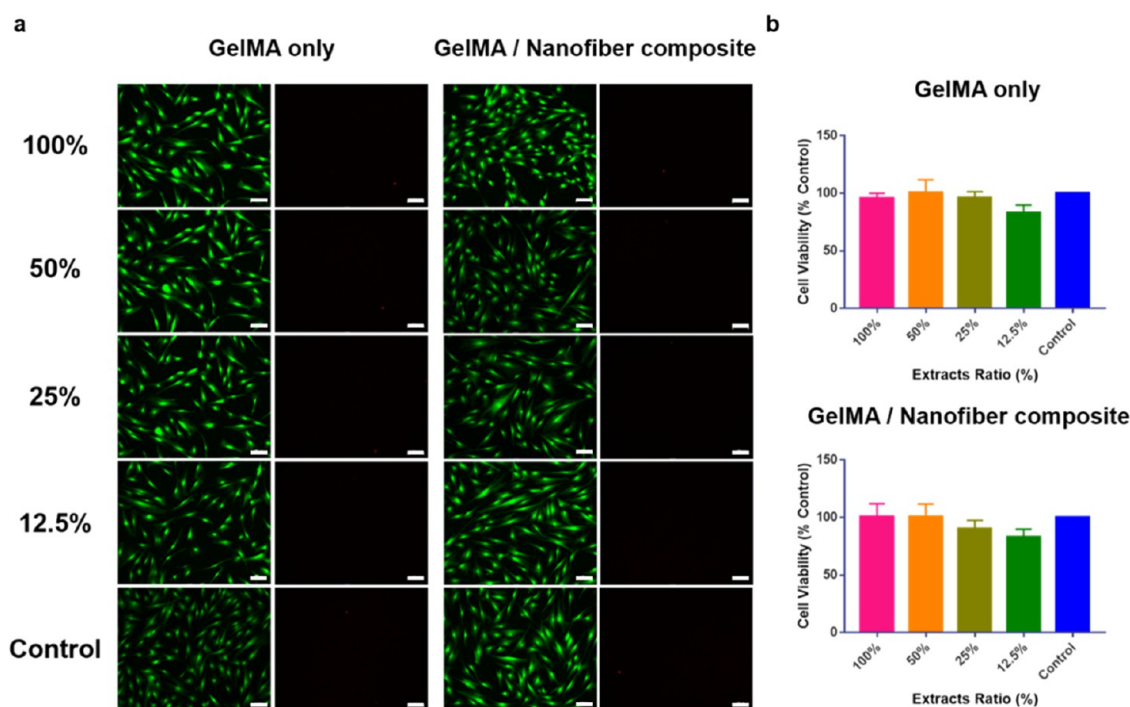

Figure 6. Cytotoxicity of the hydrogel/nanofiber composites. Fluorescent images of fibroblasts treated with GelMA or hydrogel composite extracts for 4 days and subsequently stained with live (green) and dead (red) dyes (a); cell viability of fibroblasts treated with GelMA hydrogel composite extract as determined using CCK-8 assay on day 4 (b). Data are mean ± SD. Scale bar: 100 μm.

mimicking the epidermis and dermis layer without scarring, cell arrangement and the interaction level with the cells should be considered simultaneously. Excessive myofibroblast expression during the regeneration phase can cause wound contraction and immoderate collagen production, increasing the risk of scar formation. As the ratio of gelatin increased, the expression level of α-SMA was also upregulated, which may have been attributed to increased stretching and migration from an elastic property of gelatin.

First, for the aligned 6:4 nanofibers which facilitate the regeneration of the epidermis layer of skin, the 6:4 nanofibers displayed the highest expression of α-SMA, collagen I, and collagen III, with the lowest collagen I/III ratio, a marker of scar occurrence, making it the best choice for epidermis regeneration with the least risk of scarring.

Notably, fibroblasts cultured on the interlaced nanofibers showed different expression patterns of collagen I and III than aligned nanofibers. Gene expression of collagen I was highest

at the 8:2 ratio, with a more balanced collagen I/III ratio than that of the 6:4 nanofibers. These results demonstrated that fibroblasts stayed in control over their activation *via* interactions with the surrounding environment and other cells to facilitate the wound healing process. Sin et al. also found that when the nanofiber arrangement was modified from random to aligned and crossed, the expression of fibroblasts altered, demonstrating the importance of considering cell arrangement when regenerating the dermis layer.[6] Additionally, the collagen I/III ratio of the 6:4 nanofibers was about four times higher than that of the 8:2 nanofibers, which is a similar collagen I/III ratio that can be found in keloid or hypertrophic wounds. Thus, we chose 8:2 nanofibers, as they promoted balanced cell–nanofiber interaction for scar-free dermis layer healing.

3.4. Synthesis and Characterization of the Hydrogel Composite. UV crosslinking was used to cure the hydrogel composite while keeping the GelMA precursor solution evenly
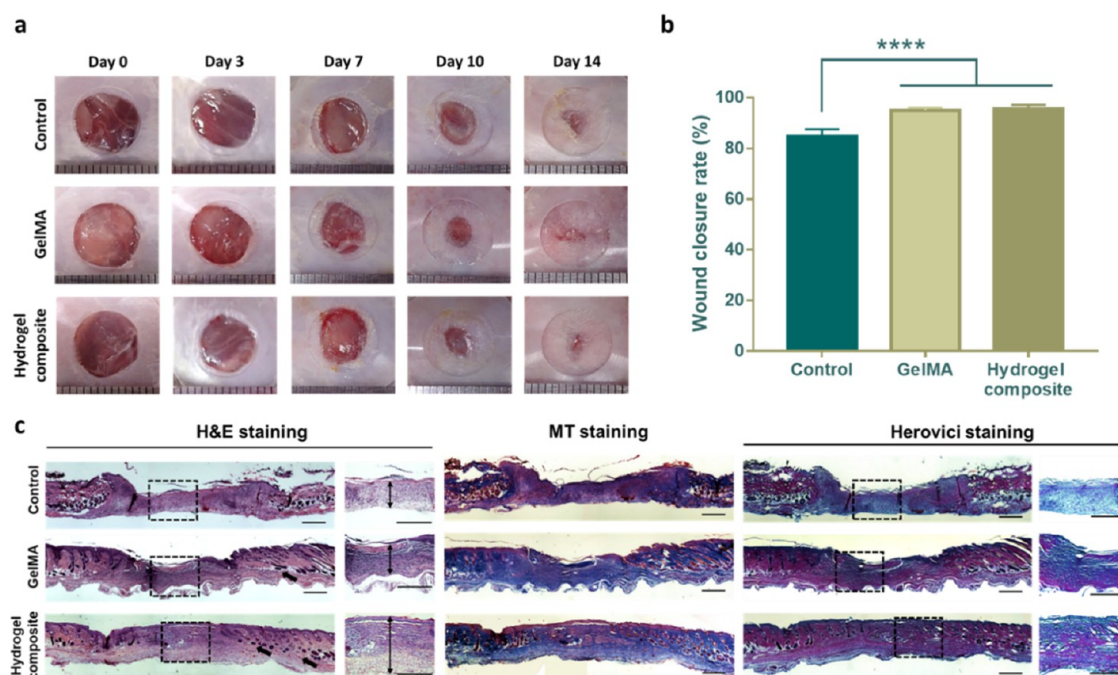
Figure 7. Digital photographs showing full-thickness wounds of control, GelMA, and hydrogel composite groups over 14 days (a); quantification of wound closure rate as determined on day 14 (b); histological evaluation of H&E-, Masson's trichrome-, and Herovici-stained skin as collected from control, GelMA, and hydrogel composite groups on day 14 (c); black arrows indicate cell migration toward the wound site. The double-headed arrows in the inset indicate the thickness of the re-epithelized wound bed. Scale bar: 500 μm (insets: 100 μm).

distributed across the nanofibers on both sides of the hydrogel solution. Following that, experiments were carried out to see if the fabricated hydrogel composite could act as a wound dressing and promote wound healing by mimicking the skin layer and directing cell growth and migration *via* mechano-transduction.

First, the rheology of the hydrogel composite was tested to ensure that it could reliably protect the wound area (Figure 5a). In the constant deformation mode, the storage modulus of the GelMA and hydrogel composites was measured at 25 °C with a deformation of 10% maintained across a frequency range of 0.1−300 Hz (rad/s). Looking at the results, the GelMA could not be used long term because it was too brittle to function as a wound dressing. Impressively, the nanofibers worked as a rigid support for the composite scaffold as they were introduced, and the overall storage modulus was approximately tripled. The resultant hydrogel composite structure had an 8000 Pa strength, which was the strength to reliably shield the wound region.

The hydrogel composite was then put through a swelling test to demonstrate that it is feasible to be used as a dressing (Figure 5b). One of the benefits of using hydrogel as a wound dressing is that it can enhance cell activation and limit microbial growth by maintaining a suitable level of moisture at the wound site. Furthermore, the hydrogel wound dressing can absorb exudate, a nutrient-rich fluid generated by the wound, which might encourage the growth of bacteria. Bacterial infection can generate a continual immunological response and promote the development of chronic wounds by forming a bacterial film on the wound surface.[1,38] Therefore, it is important to maintain an appropriate moist environment on the wound surface, and hydrogel can provide an optimal environment for skin regeneration by absorbing excess fluid through swelling. As the stiffness of the hydrogel increased, the

measured swelling ratio decreased because it was difficult to expand from its original state. As expected, the swelling ratio was higher in GelMA (654 ± 44%), and the hydrogel composite showed a lower value (533 ± 30%), possibly due to increased strength from the addition of nanofibers. However, the values measured in the hydrogel composite can also absorb exudate with a very high efficiency, exceeding 400% of its original state. In addition, the rate at which the swelling ratio reached the maximum was rapid in both groups, showing that the exudate can be effectively removed from the wound area.

3.5. Cytotoxicity Assay. Biocompatibility and cytotoxicity of the GelMA and hydrogel composite were tested by CCK-8 and Live/Dead assay using human fibroblasts (Figure 6). Human fibroblasts were subjected to the serially diluted hydrogel extracts (100, 50, 25, 12.5, and control), and their cytotoxicity was evaluated on days 1 and 4. On day 1, the viability was close to the control in all groups (Figure S8), and even on day 4, the viability was greater than 90%, indicating that the hydrogel composite was biocompatible and nontoxic. After incubation with diluted medium solution, fluorescence images of live (green) and dead (red) human fibroblasts were obtained. Almost all of the observed cells were live, while dead cells were rarely found in all diluted conditions on days 1 and 4. All cells showed a normal morphology and high viability, similar to the control group.

3.6. Evaluation of Wound Healing *In Vivo*. Wound healing on a full-thickness wound model was observed in control, GelMA, and hydrogel composite groups over 14 days. Representative images of the wounds as taken on days 0, 3, 7, 10, and 14 clearly show that the wounds of the GelMA and hydrogel composite groups healed more rapidly than that of the control group (Figure 7a). Additionally, no substantial scab formation occurred on the wound surface in the dressing-treated groups, implying less discomfort and a low chance of
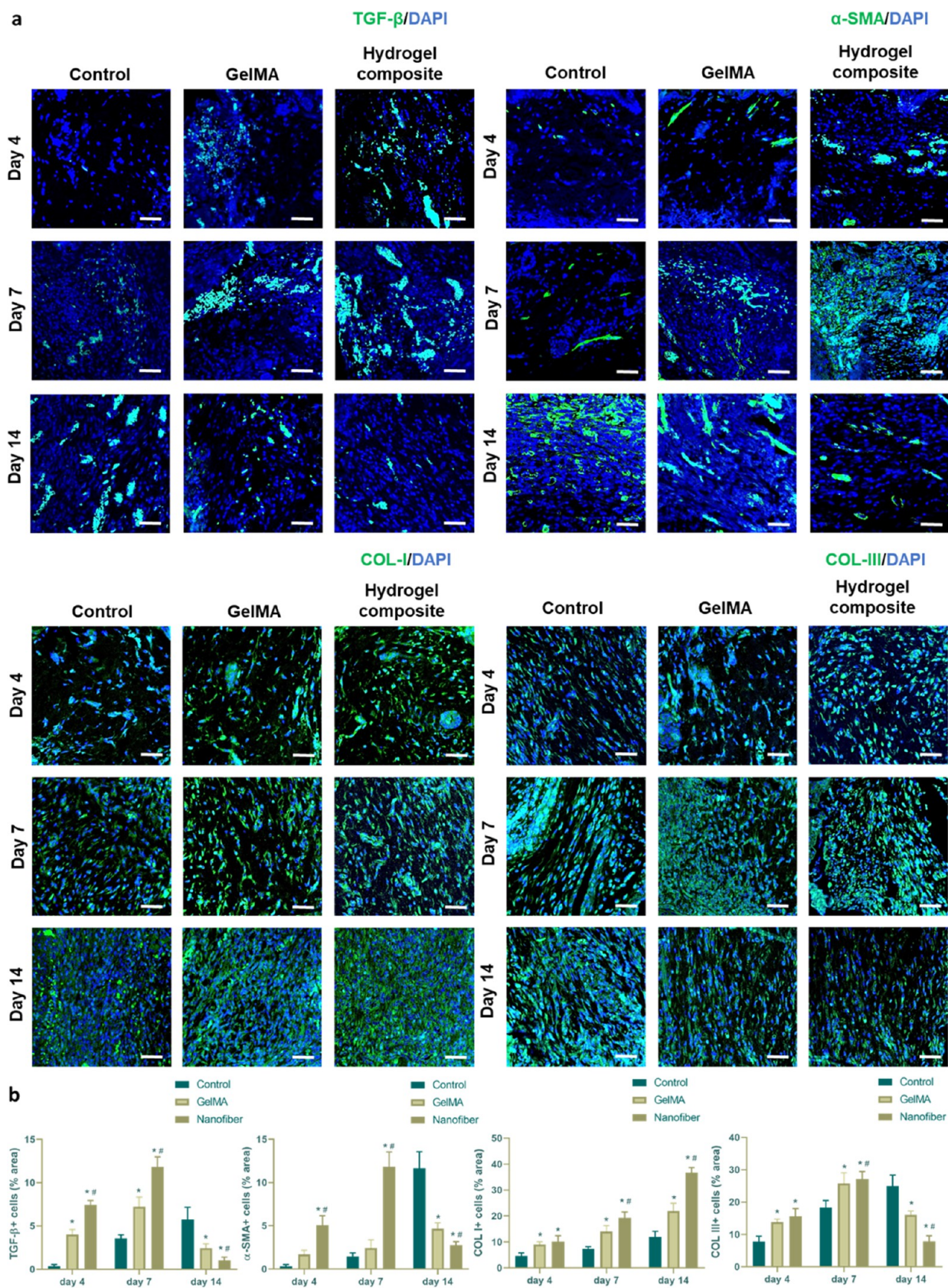
Figure 8. Immunohistochemical staining of TGF-β1, α-SMA, collagen I, and collagen III of full-thickness wounds collected on days 3, 7, and 14 (a). Scale bar: 50 μm. Quantification of TGF-β1-, α-SMA-, collagen I- and collagen III-positive cells in wounded skin as determined using ImageJ software (b). Data are mean ± SD *$p < 0.05$ against the control group; #$p < 0.05$ against GelMA group.

scarring during the wound healing process. On the 14th day, the wounds of all groups had healed significantly, but the wounds treated with the hydrogel composite had healed the most completely at about 95% (Figure 7b). Due to GelMA's superior wound healing promoting capabilities, there was no statistically significant difference in the wound healing rate between the GelMA and hydrogel composite groups. This proved that even in the presence of nanofibers, GelMA greatly promotes wound healing and can proceed with re-epithelialization, a vital step in re-establishing the protective barrier function of the skin. The role of nanofibers in the accelerated regeneration rate is to simulate the skin layer by regulating the growth and expression of cells and inducing the arrangement and composition of collagen constituting each layer. Thus, histological analysis was performed to determine whether the nanofibers had an effect on collagen production and skin layer reconstruction in comparison to the other groups during wound healing and to determine whether matrix remodeling, the most critical phase of regeneration, could be accelerated (Figure 7c).

Collagen deposition and organization are critical indications of wound healing extent. After 14 days, the mice were sacrificed, and histological assessment on collected skin was performed by H&E, Masson's trichrome, and Herovici staining to determine the hydrogel composite's therapeutic potential. The findings of the H&E staining revealed that all groups exhibited varying levels of cell migration and proliferation, all of which contributed to the regeneration of granulation tissue. In comparison to the other groups, the hydrogel composite significantly accelerated wound healing by encouraging cell migration and proliferation, demonstrating the nanofibers' cell activation enhancing function, as indicated by the black arrow in Figure 7c. Histological analysis in Figure S9 revealed that the hydrogel composite group resulted in a faster onset of re-epitheilization, as indicated by the thin line of re-epithelized bed, compared to little re-epithelialization observed in the GelMA and control groups at day 4. At day 7, the hydrogel composite group formed thicker granulation tissue than the GelMA group, with the control group still having an incomplete lining of the re-epithelized bed. On day 14, all three groups formed granulation tissues that completely covered the wounded area, with the hydrogel composite group having the thickest re-epithelialized bed, followed by GelMA and then by the control group. Remarkably, the architecture of the epidermis and dermis skin layers was astonishingly well regenerated in the hydrogel composite group, but in the other groups, the granulation process seemed to be still ongoing. These findings supported our conclusion that our nanofiber dressing accelerated the proliferative phase of fibroblasts to promote the wound healing process. Then, Masson's trichrome staining showed newly deposited collagen in the regenerated skin. The results revealed that wound beds from the GelMA group and hydrogel composite group were completely covered with newly deposited collagen, while the control group deposited comparably less collagen. However, Herovici staining revealed that the hydrogel composite stimulated the greatest quantity of mature collagen formation on the regenerated skin when compared to normal skin (Figure S10).

3.7. Immunofluorescent Staining of Skin. Quantitative study of immunohistochemical staining revealed correlating results with histological analysis (Figure 8). First, TGF-β1, a factor that regulates the immune response and granular tissue production in early time points, was at its peak in the hydrogel composite group on days 3 and 7 and then significantly decreased on day 14. TGF-β1 induces the recruitment of inflammatory cells, including leukocytes, monocytes, and macrophages, to the site of damage to promote an initial immune response.[39] In addition, TGF-β1 stimulates the production of ECM proteins, including fibronectin, collagen I and III, and VEGF, which stimulates granular tissue synthesis.[40] Furthermore, TGF-β1 enhances the angiogenic capabilities of endothelial progenitor cells to increase blood flow to the wounded location and promotes the contraction of fibroblasts to promote wound healing.[41] On the basis of this effectiveness, increased expression of TGF-β1 during the early phase of wound healing can promote wound healing. On the contrary, overexpression of TGF-β1 can lead to the formation of scars through its stimulatory effects on the expression of essential ECM components and its inhibitory effects on the production of MMP.[42] The considerable reduction in TGF-β1 expression on day 14 in the hydrogel composite group indicates that the hydrogel composite can inhibit the formation of a chronic or hypertrophic wound and promote normal repair. Next, the expression levels of α-SMA, a marker of myofibroblasts, were examined. The number of α-SMA-positive cells exhibited the same pattern as that of TGF-β1, which was expected, as TGF-β1 stimulates migration of fibroblast and differentiation into myofibroblast.[43] Myofibroblasts are cells that differentiate from fibroblasts in response to mechanical and biological stimuli; they are a primary producer of collagen I and generate α-SMA and assist in wound contraction. Surprisingly, on day 14, the expression level of α-SMA$^+$ cells was the lowest in the hydrogel composite group, indicating that the hydrogel composite could inhibit keloid and hypertrophic scarring caused by excessive mechanical tension. Interestingly, by day 14, the expression level of collagen III in the hydrogel composite was reduced, whereas the expression level of collagen I, also known as mature collagen, which substitutes III collagen through matrix remodeling, rose significantly. This demonstrated that fibroblasts arranged in the same manner as natural skin under the guidance of nanofibers in a hydrogel composite could rapidly induce the arrangement of collagen during wound healing, thereby promoting the expression of mature collagen I. The expression of α-SMA and the ratio of Col I/III were maintained at normal skin levels on day 14. This implies that the hydrogel composite promotes wound healing, inhibits scar formation, and has a structure and composition that resembles the natural skin layer. These results are consistent with our paper's goal, which is to promote skin regeneration and pursue wound healing with a good prognosis similar to normal skin using nanofibers to modulate cell activity during the regeneration process (Figure S10). Taken together, our results indicate that the hydrogel composite group exhibited superior wound healing potential than the other two groups.

4. CONCLUSIONS

In this study, we successfully fabricated hydrogel/nanofiber composite wound dressings with a fine-tuned composition and arrangement of nanofibers that can modulate the bioactivities of cells that participate in wound healing. An *in vitro* test was used to validate the hydrogel composite's functionality and potential to control cell expression as a wound dressing. Additionally, the effects of the hydrogel composite on wound healing were thoroughly investigated using full-thickness

wound models. *In vivo* experiments demonstrated that the hydrogel composites could not only enhance wound contraction by rapid re-epithelialization but also significantly accelerate the matrix remodeling process, which has a substantial effect on the prognosis. Our findings show the possibility of an advanced wound dressing that promotes wound healing in an integrated manner without the need for biological medication.

■ ASSOCIATED CONTENT

ⓢ Supporting Information

The Supporting Information is available free of charge at https://pubs.acs.org/doi/10.1021/acsabm.3c00014.

Digital photograph of a hydrogel composite wound dressing (Figure S1); primer sequences used for qRT-PCR gene expression analysis (Figure S2); list of antibodies used in the study (Figure S3); characterization of the nanofibrous scaffolds (Figure S4); characterization of the interlaced nanofibers, SEM images of the 8:2 interlaced nanofibers showing a smooth surface without beading or branching (a), orientation coherency analysis of the 8:2 interlaced nanofibers (b), scale bar: 150 μm (Figure S5); fluorescent images showing the morphology of macrophages and keratinocytes cultured on the nanofiber scaffolds for 24 h, F-actin (red) of (a) Macrophage, (b) Keratinocyte was stained with ActinRed 555 ReadyProbes (Invitrogen, Waltham, MA), scale bar: 100 μm (Figure S6); changes in gene expression of fibroblasts cultured on nanofibers with varying PCL/gelatin ratios, fibroblasts were cultured on aligned and interlaced nanofibrous scaffold with varying PCL/gelatin ratios for 1 day, and its gene expression was analyzed by qRT-PCR; all values were normalized to GAPDH, data are mean ± SD (Figure S7); cytotoxicity of the hydrogel/nanofiber composites, fluorescent images of fibroblasts treated with GelMA or hydrogel composite extracts for 1 day and subsequently stained with live (green) and dead (red) dyes (a), cell viability of fibroblasts treated with GelMA hydrogel composite extract as determined using CCK-8 assay on day 1 (b), data are mean ± SD, scale bar: 100 μm (Figure S8); histological evaluation of H&E- and Masson's trichrome-stained skin as collected from the control, GelMA, and hydrogel composite groups on day 4 and 7 (Figure S9); histological analysis of normal skin, histological evaluation of H&E-, Masson's trichrome-, and Herovici-stained skin of normal skin, scale bar: 500 μm (a); immunohistochemical staining of TGF-β1, α-SMA, collagen I, and collagen III of normal skin, scale bar: 50 μm (b); quantification of TGF-β1, α-SMA, collagen I, and collagen III-positive cells in normal skin as determined using imageJ software (c) (Figure 10) (PDF)

■ AUTHOR INFORMATION

Corresponding Authors

Sang-Heon Kim − *Center for Biomaterials, Biomedical Research Institute, Korea Institute of Science and Technology (KIST), Seoul 02792, Republic of Korea; Division of Bio-Medical Science and Technology, KIST School, University of Science and Technology, Seoul 02792, Republic of Korea;* Email: skimbrc@kist.re.kr

Kangwon Lee − *Department of Applied Bioengineering, Research Institute for Convergence Science, Seoul National University, Seoul 08826, Republic of Korea; Research Institute for Convergence Science, Seoul National University, Seoul 08826, Republic of Korea;* ⓘ orcid.org/0000-0001-5745-313X; Email: kangwonlee@snu.ac.kr

Authors

Changgi Hong − *Department of Applied Bioengineering, Research Institute for Convergence Science, Seoul National University, Seoul 08826, Republic of Korea;* ⓘ orcid.org/0000-0003-4324-1392

Haeun Chung − *Center for Biomaterials, Biomedical Research Institute, Korea Institute of Science and Technology (KIST), Seoul 02792, Republic of Korea; Division of Bio-Medical Science and Technology, KIST School, University of Science and Technology, Seoul 02792, Republic of Korea*

Gyubok Lee − *Department of Applied Bioengineering, Research Institute for Convergence Science, Seoul National University, Seoul 08826, Republic of Korea;* ⓘ orcid.org/0000-0001-6634-7523

Changheon Kim − *Program in Nanoscience and Technology, Department of Applied Bioengineering, Research Institute for Convergence Science, Seoul National University, Seoul 08826, Republic of Korea;* ⓘ orcid.org/0000-0002-5451-0853

Dongwoo Kim − *Department of Applied Bioengineering, Research Institute for Convergence Science, Seoul National University, Seoul 08826, Republic of Korea*

Seung Ja Oh − *Center for Biomaterials, Biomedical Research Institute, Korea Institute of Science and Technology (KIST), Seoul 02792, Republic of Korea; Division of Bio-Medical Science and Technology, KIST School, University of Science and Technology, Seoul 02792, Republic of Korea*

Complete contact information is available at:
https://pubs.acs.org/10.1021/acsabm.3c00014

Author Contributions

#C.H. and H.C. indicates first authors. C.H.: conceptualization, methodology, data curation, visualization, writing—original draft, and writing—review & editing. H.C.: data analysis, investigation, methodology, visualization, and writing—review & editing. G.L.: resources and formal analysis. C.K.: data curation and writing—review & editing. D.K.: software and validation. S.J.O.: data curation. S.-H.K.: supervision and funding acquisition. K.L.: supervision, funding acquisition, and project administration.

Notes

The authors declare no competing financial interest.

■ ACKNOWLEDGMENTS

■ REFERENCES

(1) Liang, Y. P.; He, J. H.; Guo, B. L. Functional Hydrogels as Wound Dressing to Enhance Wound Healing. *ACS Nano* **2021**, *15*, 12687−12722.

(2) Zeng, Q. K.; Qi, X. L.; Shi, G. Y.; Zhang, M.; Haick, H. Wound Dressing: From Nanomaterials to Diagnostic Dressings and Healing Evaluations. *ACS Nano* **2022**, *16*, 1708−1733.

(3) Gaspar-Pintiliescu, A.; Stanciuc, A. M.; Craciunescu, O. Natural composite dressings based on collagen, gelatin and plant bioactive compounds for wound healing: A review. *Int. J. Biol. Macromol.* **2019**, *138*, 854−865.

(4) Jayakumar, R.; Prabaharan, M.; Kumar, P. T. S.; Nair, S. V.; Tamura, H. Biomaterials based on chitin and chitosan in wound dressing applications. *Biotechnol. Adv.* **2011**, *29*, 322−337.

(5) Zhong, Y. J.; Xiao, H. N.; Seidi, F.; Jin, Y. C. Natural Polymer-Based Antimicrobial Hydrogels without Synthetic Antibiotics as Wound Dressings. *Biomacromolecules* **2020**, *21*, 2983−3006.

(6) Sun, L.; Gao, W.; Fu, X.; Shi, M.; Xie, W.; Zhang, W.; Zhao, F.; Chen, X. Enhanced wound healing in diabetic rats by nanofibrous scaffolds mimicking the basketweave pattern of collagen fibrils in native skin. *Biomater. Sci.* **2018**, *6*, 340−349.

(7) Fares, M. M.; Sani, E. S.; Lara, R. P.; Oliveira, R. B.; Khademhosseini, A.; Annabi, N. Interpenetrating network gelatin methacryloyl (GelMA) and pectin-g-PCL hydrogels with tunable properties for tissue engineering. *Biomater. Sci.* **2018**, *6*, 2938−2950.

(8) Han, N.; Xu, Z.; Cui, C.; Li, Y.; Zhang, D.; Xiao, M.; Fan, C.; Wu, T.; Yang, J.; Liu, W. A Fe(3+)-crosslinked pyrogallol-tethered gelatin adhesive hydrogel with antibacterial activity for wound healing. *Biomater. Sci.* **2020**, *8*, 3164−3172.

(9) Augustine, R.; Zahid, A. A.; Hasan, A.; Dalvi, Y. B.; Jacob, J. Cerium Oxide Nanoparticle-Loaded Gelatin Methacryloyl Hydrogel Wound-Healing Patch with Free Radical Scavenging Activity. *ACS Biomater. Sci. Eng.* **2021**, *7*, 279−290.

(10) Fares, M. M.; Sani, E. S.; Lara, R. P.; Oliveira, R. B.; Khademhosseini, A.; Annabi, N. Interpenetrating network gelatin methacryloyl (GelMA) and pectin-g-PCL hydrogels with tunable properties for tissue engineering. *Biomater. Sci.* **2018**, *6*, 2938−2950.

(11) Mahjour, S. B.; Sefat, F.; Polunin, Y.; Wang, L.; Wang, H. Improved cell infiltration of electrospun nanofiber mats for layered tissue constructs. *J. Biomed. Mater. Res., Part A* **2016**, *104*, 1479−1488.

(12) Omidinia-Anarkoli, A.; Boesveld, S.; Tuvshindorj, U.; Rose, J. C.; Haraszti, T.; De Laporte, L. An Injectable Hybrid Hydrogel with Oriented Short Fibers Induces Unidirectional Growth of Functional Nerve Cells. *Small* **2017**, *13*, No. 1702207.

(13) Xu, Y.; Shi, G.; Tang, J.; Cheng, R.; Shen, X.; Gu, Y.; Wu, L.; Xi, K.; Zhao, Y.; Cui, W.; Chen, L. ECM-inspired micro/nanofibers for modulating cell function and tissue generation. *Sci. Adv.* **2020**, *6*, No. eabc2036.

(14) Luu, T. U.; Gott, S. C.; Woo, B. W.; Rao, M. P.; Liu, W. F. Micro- and Nanopatterned Topographical Cues for Regulating Macrophage Cell Shape and Phenotype. *ACS Appl. Mater. Interfaces* **2015**, *7*, 28665−28672.

(15) McWhorter, F. Y.; Wang, T.; Nguyen, P.; Chung, T.; Liu, W. F. Modulation of macrophage phenotype by cell shape. *Proc. Natl. Acad. Sci. U.S.A.* **2013**, *110*, 17253−17258.

(16) Pal, P.; Dadhich, P.; Srivas, P. K.; Das, B.; Maulik, D.; Dhara, S. Bilayered nanofibrous 3D hierarchy as skin rudiment by emulsion electrospinning for burn wound management. *Biomater. Sci.* **2017**, *5*, 1786−1799.

(17) Rho, K. S.; Jeong, L.; Lee, G.; Seo, B. M.; Park, Y. J.; Hong, S. D.; Roh, S.; Cho, J. J.; Park, W. H.; Min, B. M. Electrospinning of collagen nanofibers: effects on the behavior of normal human keratinocytes and early-stage wound healing. *Biomaterials* **2006**, *27*, 1452−1461.

(18) Loessner, D.; Meinert, C.; Kaemmerer, E.; Martine, L. C.; Yue, K.; Levett, P. A.; Klein, T. J.; Melchels, F. P.; Khademhosseini, A.; Hutmacher, D. W. Functionalization, preparation and use of cell-laden gelatin methacryloyl-based hydrogels as modular tissue culture platforms. *Nat. Protoc.* **2016**, *11*, 727−746.

(19) Li, Z.; Zhou, F.; Li, Z.; Lin, S.; Chen, L.; Liu, L.; Chen, Y. Hydrogel Cross-Linked with Dynamic Covalent Bonding and Micellization for Promoting Burn Wound Healing. *ACS Appl. Mater. Interfaces* **2018**, *10*, 25194−25202.

(20) Choi, Y.; Park, M. H.; Lee, K. Injectable thermoresponsive hydrogel/nanofiber hybrid scaffolds inducing human adipose-derived stem cell chemotaxis. *J. Ind. Eng. Chem.* **2020**, *82*, 89−97.

(21) Gao, L. L.; Chen, J. J.; Feng, W.; Song, Q.; Huo, J. J.; Yu, L. F.; Liu, N.; Wang, T. J.; Li, P.; Huang, W. A multifunctional shape-adaptive and biodegradable hydrogel with hemorrhage control and broad-spectrum antimicrobial activity for wound healing. *Biomater. Sci.* **2020**, *8*, 6930−6945.

(22) Cook, K. A.; Naguib, N.; Kirsch, J.; Hohl, K.; Colby, A. H.; Sheridan, R.; Rodriguez, E. K.; Nazarian, A.; Grinstaff, M. W. In situ gelling and dissolvable hydrogels for use as on-demand wound dressings for burns. *Biomater. Sci.* **2021**, *9*, 6842−6850.

(23) Suo, H. R.; Zhang, D. M.; Yin, J.; Qian, J.; Wu, Z. L.; Fu, J. Z. Interpenetrating polymer network hydrogels composed of chitosan and photocrosslinkable gelatin with enhanced mechanical properties for tissue engineering. *Mater. Sci. Eng.: C* **2018**, *92*, 612−620.

(24) Usal, T. D.; Yucel, D.; Hasirci, V. A novel GelMA-pHEMA hydrogel nerve guide for the treatment of peripheral nerve damages. *Int. J. Biol. Macromol.* **2019**, *121*, 699−706.

(25) Arica, T. A.; Guzelgulgen, M.; Yildiz, A. A.; Demir, M. M. Electrospun GelMA fibers and p(HEMA) matrix composite for corneal tissue engineering. *Mater. Sci. Eng., C* **2021**, *120*, No. 111720.

(26) Shirazi, A. N.; Fathi, A.; Suarez, F. G.; Wang, Y.; Maitz, P. K.; Dehghani, F. A Novel Strategy for Softening Gelatin-Bioactive-Glass Hybrids. *ACS Appl. Mater. Interfaces* **2016**, *8*, 1676−1686.

(27) Gautam, S.; Dinda, A. K.; Mishra, N. C. Fabrication and characterization of PCL/gelatin composite nanofibrous scaffold for tissue engineering applications by electrospinning method. *Mater. Sci. Eng., C* **2013**, *33*, 1228−1235.

(28) Goudarzi, Z. M.; Behzad, T.; Ghasemi-Mobarakeh, L.; Kharaziha, M. An investigation into influence of acetylated cellulose nanofibers on properties of PCL/Gelatin electrospun nanofibrous scaffold for soft tissue engineering. *Polymer* **2021**, *213*, No. 123313.

(29) Ren, K.; Wang, Y.; Sun, T.; Yue, W.; Zhang, H. Y. Electrospun PCL/gelatin composite nanofiber structures for effective guided bone regeneration membranes. *Mater. Sci. Eng., C* **2017**, *78*, 324−332.

(30) Osman, O. S.; Selway, J. L.; Harikumar, P. E.; Stocker, C. J.; Wargent, E. T.; Cawthorne, M. A.; Jassim, S.; Langlands, K. A novel method to assess collagen architecture in skin. *BMC Bioinf.* **2013**, *14*, No. 260.

(31) van Zuijlen, P. P.; Ruurda, J. J.; van Veen, H. A.; van Marle, J.; van Trier, A. J.; Groenevelt, F.; Kreis, R. W.; Middelkoop, E. Collagen morphology in human skin and scar tissue: no adaptations in response to mechanical loading at joints. *Burns* **2003**, *29*, 423−431.

(32) Kechagia, J. Z.; Ivaska, J.; Roca-Cusachs, P. Integrins as biomechanical sensors of the microenvironment. *Nat. Rev. Mol. Cell Biol.* **2019**, *20*, 457−473.

(33) Dupont, S.; Morsut, L.; Aragona, M.; Enzo, E.; Giulitti, S.; Cordenonsi, M.; Zanconato, F.; Le Digabel, J.; Forcato, M.; Bicciato, S.; Elvassore, N.; Piccolo, S. Role of YAP/TAZ in mechanotransduction. *Nature* **2011**, *474*, 179−183.

(34) Dobrokhotov, O.; Samsonov, M.; Sokabe, M.; Hirata, H. Mechanoregulation and pathology of YAP/TAZ via Hippo and non-Hippo mechanisms. *Clin. Transl. Med.* **2018**, *7*, No. e23.

(35) Lee, M. J.; Byun, M. R.; Furutani-Seiki, M.; Hong, J. H.; Jung, H. S. YAP and TAZ regulate skin wound healing. *J. Invest. Dermatol.* **2014**, *134*, 518−525.

(36) Chen, H.; Lui, Y. S.; Tan, Z. W.; Lee, J. Y. H.; Tan, N. S.; Tan, L. P. Migration and Phenotype Control of Human Dermal Fibroblasts by Electrospun Fibrous Substrates. *Adv. Healthcare Mater.* **2019**, *8*, No. 1801378.

(37) Jia, Y.; Yang, W.; Zhang, K.; Qiu, S.; Xu, J.; Wang, C.; Chai, Y. Nanofiber arrangement regulates peripheral nerve regeneration through differential modulation of macrophage phenotypes. *Acta Biomater.* **2019**, *83*, 291−301.

(38) Wang, K.; Wang, J. H.; Li, L.; Xu, L. Q.; Feng, N.; Wang, Y.; Fei, X.; Tian, J.; Li, Y. Novel Nonreleasing Antibacterial Hydrogel Dressing by a One-Pot Method. *ACS Biomater. Sci. Eng.* **2020**, *6*, 1259−1268.

(39) Pakyari, M.; Farrokhi, A.; Maharlooei, M. K.; Ghahary, A. Critical Role of Transforming Growth Factor Beta in Different Phases of Wound Healing. *Adv. Wound Care* **2013**, *2*, 215−224.

(40) Bettinger, D. A.; Yager, D. R.; Diegelmann, R. F.; Cohen, I. K. The effect of TGF-beta on keloid fibroblast proliferation and collagen synthesis. *Plast. Reconstr. Surg.* **1996**, *98*, 827−833.

(41) Ferrari, G.; Cook, B. D.; Terushkin, V.; Pintucci, G.; Mignatti, P. Transforming growth factor-beta 1 (TGF-beta1) induces angiogenesis through vascular endothelial growth factor (VEGF)-mediated apoptosis. *J. Cell. Physiol.* **2009**, *219*, 449−458.

(42) Schmid, P.; Itin, P.; Cherry, G.; Bi, C.; Cox, D. A. Enhanced expression of transforming growth factor-beta type I and type II receptors in wound granulation tissue and hypertrophic scar. *Am. J. Pathol.* **1998**, *152*, 485−493.

(43) Darby, I. A.; Laverdet, B.; Bonte, F.; Desmouliere, A. Fibroblasts and myofibroblasts in wound healing. *Clin., Cosmet. Invest. Dermatol.* **2014**, *7*, 301−311.